Exhibit C

Accepted Manuscript

Characterization of the host inflammatory response following implantation of prolapse mesh in rhesus macaque

Bryan N. Brown, PhD, Deepa Mani, MBBS, Ms. Alexis L. Nolfi, BS, Rui Liang, MD, Steve Abramowitch, PhD, Pamela A. Moalli, MD PhD

PII: S0002-9378(15)00853-4

DOI: 10.1016/j.ajog.2015.08.002

Reference: YMOB 10566

To appear in: *American Journal of Obstetrics and Gynecology*

Received Date: 15 April 2015

Revised Date: 21 June 2015

Accepted Date: 2 August 2015

Please cite this article as: Brown BN, Mani D, Nolfi AL, Liang R, Abramowitch S, Moalli PA, Characterization of the host inflammatory response following implantation of prolapse mesh in rhesus macaque, *American Journal of Obstetrics and Gynecology* (2015), doi: 10.1016/j.ajog.2015.08.002.

Characterization of the host inflammatory response following implantation of prolapse mesh in rhesus macaque

Bryan N. Brown, PhD[1,2,3], Deepa Mani, MBBS[3], Ms. Alexis L. Nolfi, BS[1], Rui Liang[2,4] MD, Steve Abramowitch PhD[1, 2], and Pamela A. Moalli, MD PhD[1,2,3,4,*]

1. Department of Bioengineering, University of Pittsburgh
2. Department of Obstetrics, Gynecology, and Reproductive Sciences, University of Pittsburgh
3. McGowan Institute for Regenerative Medicine, University of Pittsburgh
4. Magee Womens Research Institute

Study was conducted in Pittsburgh, PA, USA

The Authors Report No Conflict of Interest

This work was supported by National Institutes of Health awards R01 HD061811 (P.A.M) and K12HD043441 (B.N.B). The content is solely the responsibility of the authors and does not necessarily represent the official views of the National Institutes of Health. The funding source had no involvement in the study design, collection of data, analysis of data, interpretation of data, writing of the report, or the decision to submit for publication.

These findings were presented at the 2014 American Urogynecologic Society/International Urogynecologic Association Joint Scientific Meeting in Washington, DC, July 22-26th, 2014.

*To Whom Correspondence Should Be Addressed:
Dr. Pamela A. Moalli
Magee-Womens Research Institute
204 Craft Ave
Pittsburgh, PA 15213
Tel: 412-641-6052
Email: pmoalli@mail.magee.edu

Word Count
Abstract: 350 Main Text: 3350

CONDENSATION

The inflammatory response to mesh consists primarily of macrophages polarized towards a pro-inflammatory M1 phenotype which is dependent upon mesh textile properties and mesh burden.

SHORT VERSION OF TITLE

Inflammatory Response to Prolapse Mesh.

ABSTRACT

Objective: To determine the predominant cell type (macrophage, T-lymphocyte, B-lymphocyte, mast cell) within the area of implantation of the prototypical polypropylene mesh, Gynemesh PS (Ethicon); and to determine the phenotypic profile (M1 pro-inflammatory, M2 anti-inflammatory) of the macrophage response to three different polypropylene meshes: Gynemesh PS (Ethicon), and two lower weight, higher porosity meshes, UltraPro (Ethicon) and Restorelle (Coloplast).

Study Design: Sacrocolpopexy was performed following hysterectomy in rhesus macaques. Sham-operated animals served as controls. At 12 weeks post-surgery, the vagina-mesh complex was excised and the host inflammatory response was evaluated. Hematoxylin and eosin was used to perform routine histomorphologic evaluation. Identification of leukocyte (CD45+) subsets was performed by immunolabeling for CD68 (macrophage), CD3 (T-lymphocyte), CD20 (B-lymphocyte), and CD117 (mast cell). M1 and M2 macrophage subsets were identified using immunolabeling (CD86+ and CD206+, respectively), and further evaluation was performed using ELISA for two M1 (TNF-α and IL-12) and two M2 (IL-4 and IL-10) cytokines.

Results: Histomorphologic evaluation showed a dense cellular response surrounding each mesh fiber. CD45+ leukocytes accounted for 21.4±5.4% of total cells within the peri-mesh area captured in a 20X field, with macrophages as the predominant luekocyte subset (10.5±3.9% of total cells) followed by T-lymphocytes (7.3±1.7%), B-lymphocytes (3.0±1.2%), and mast cells (0.2±0.2%). The response was observed to be more diffuse with increasing distance from the fiber surface. Few leukocytes of any type were observed in sham-operated animals. Immunolabeling revealed polarization of the macrophage response towards the M1 phenotype in

all mesh groups. However, the ratio of M2:M1 macrophages was increased in the fiber area in UltraPro (P=0.033) and Restorelle (P=0.016) compared to Gynemesh PS. In addition, a shift towards increased expression of the anti-inflammatory cytokine IL-10 was observed in Restorelle as compared to Gynemesh PS (P=0.011).

Conclusions: The host response to mesh consists predominantly of activated, pro-inflammatory, M1 macrophages at 12 weeks post-surgery. However, this response is attenuated with implantation of lighter weight, higher porosity mesh. While additional work is required to establish causal relationships, these results suggest a link between the host inflammatory response, mesh textile properties, and clinical outcomes in the repair of pelvic organ prolapse.

Keywords: cytokines, inflammatory response, macrophage phenotype, polypropylene mesh, rhesus macaque

INTRODUCTION

More than 250,000 women per year in the United States will undergo surgery for the treatment of pelvic organ prolapse, with direct costs totaling more than $1 billion.[1-3] Native tissue repair has a recurrence rate of 40% at 2 years;[4,5] therefore, mechanical reinforcement of tissues using synthetic mesh has increased over the last decade.[6] While mesh implantation has been shown improve anatomical outcomes in the anterior and apical compartments, complications are observed, particularly with transvaginal placement,[7-11] including mesh exposure through the vaginal wall, shrinkage, erosion, and pain.

Recent work suggests that mesh exposures may be induced by stress shielding. That is, a mismatch in stiffness between the mesh and tissue lead to degeneration of the underlying vagina and a loss of mechanical integrity over time. This maladaptive remodeling response precipitates atrophy of the smooth muscle layer associated with a decrease in contractility as well as a shift in tissue extracellular matrix composition and a loss of biomechanical integrity.[12-14] Differences in mesh properties (weight, pore size, porosity, stiffness) were shown to be related to the degree to which this degenerative process occurs, with higher weight, lower porosity, and increased stiffness mesh being associated with increased vaginal tissue degradation. Mesh with higher weight, lower porosity, and increased stiffness has also been suggested to result in increased rates of complications in clinical practice.[15,16]

Mesh complications may also be attributable to the inflammatory processes associated with the macrophage predominated foreign body reaction mounted by the host following implantation. Without question, the long-term presence of activated pro-inflammatory cells can have a negative impact upon the ability of a material to function as intended. However, a number of recent studies have demonstrated that the macrophage response is also an essential component

of the process leading to tissue incorporation, and functional remodeling of implanted materials suggesting the potential for phenotypic dichotomy in the host response. [17,18] Indeed, macrophages have been classified as having diverse and plastic phenotypes along a continuum between M1 (classically activated; pro-inflammatory) and M2 (alternatively activated; regulatory, homeostatic) extremes. [19-21] An increasing number of studies in the field of biomaterials have begun to apply these paradigms and concepts, showing that macrophage polarization is a predictor of integration following implantation in multiple applications. [18,22-25] However, the macrophage response following implantation of surgical mesh with varying characteristics has not been described. Moreover, limited studies to date have addressed the impact of mesh implantation on the vagina – an organ with an immunologically distinct environment from that of other tissues in which the host response to mesh has been examined.

The objectives of the present study were two-fold: (1) to determine the predominant cell type (macrophage, T-lymphocyte, B-lymphocyte, mast cell) within the area of implantation of the prototypical polypropylene mesh, Gynemesh PS (Ethicon); and (2) to determine the phenotypic profile (M1 pro-inflammatory, M2 anti-inflammatory) of the macrophage response to three different polypropylene meshes: Gynemesh PS (Ethicon), and two lower weight, higher porosity meshes, UltraPro (Ethicon) and Restorelle (Coloplast).

MATERIALS AND METHODS

Meshes

The test articles consisted of three polypropylene meshes with varying textile and mechanical characteristics as previously described. [12,26] Briefly, specific weight and pore size were provided by the manufacturer. Porosity was determined using a custom designed Matlab

algorithm (Matlab Version 8.0, Natick, MA, USA) and stiffness was determined by ball burst testing. Table 1 shows the relevant mechanical and structural characteristics associated with each mesh. Of note, UltraPro is manufactured with an absorbable component (poliglecaprolactone 25) in addition to polypropylene allowing it to have very large pores (4mm) when this component is fully absorbed.

Animals

The samples for the present study were obtained from a larger study. [12,13] A subset of animals from that study was selected based upon the availability of sufficient tissue samples for completion of the assays described in the present study. All animals in this study were maintained and treated according to an approved Institutional Animal Care and Use Committee (IACUC) protocol and in accordance with the National Institutes of Health Guide for the Care and Use of Laboratory Animals. Demographic data of each animal were collected prior to surgery, including age, weight, gravidity and parity (Table 2). Thirty-two middle-aged parous rhesus macaques underwent implantation with Gynemesh PS (n = 8), UltraPro (n = 8), Restorelle (n=8) or Sham (n=8). Mesh was implanted by sacrocolpopexy after an abdominal hysterectomy as previously described. [12,13] Sacrocolpopexy was chosen as observational data suggests that complications related to this procedure are less than those following transvaginal implantation. [11,27]

Sample Harvest

At 12 weeks post-surgery, vagina-mesh tissue complexes were harvested as previously described. [12,13] The equivalent tissues were excised in sham-operated animals. A portion of the

vagina-mesh complex was embedded in OCT prior to flash freezing on liquid nitrogen for histologic staining and immunofluorescent labeling. Another portion was harvested and frozen for ELISA assay. All samples were stored at -80°C until testing.

Histologic Staining and Immunofluorescent Labeling

Tissue sections (7μm) were cut and stored at -80°C until use. Slides were thawed at room temperature, and stained with hematoxylin and eosin. Slides were dehydrated through a series of graded ethanol (70%-100%) and xylenes prior to coverslipping. The histologic appearance of the tissue sections was then evaluated and imaged using a Nikon E600 microscope (Nikon, Melville, New York).

For immunolabeling, sections were fixed in 50:50 methanol/acetone for 10 min. Antigen retrieval was performed in 10mM citric acid monohydrate buffer (pH 6.0) at 95°C for 20 min. After cooling, the sections were incubated in copper sulfate with ammonium acetate for 20 min at 37°C to reduce autofluorescence. The sections were blocked with 1% normal donkey serum, 2% bovine serum albumin, 0.1% Triton-X100 and 0.1% Tween 20 at room temperature for 1 hour. Consecutive sections were then labeled with antibodies specific for leukocytes (CD45), macrophages (CD68), T lymphocytes (CD3), B lymphocytes (CD20), and mast cells (CD117). Primary antibodies, diluted in blocking solution, were applied overnight at 4°C, followed by the corresponding secondary antibodies (product information and dilutions for each primary and secondary antibody are listed in Supplemental Table 1) and then coverslipped using aqueous mounting media containing DAPI (Vectashield with DAPI, Vector Laboratories, Burlingame, CA). Localization of staining to the appropriate regions of lung, liver, kidney, spleen, lymph node and intestine were used to verify appropriate labeling and incubation of slides without

primary antibodies was used as a control. Three representative areas of the mesh-tissue interface were imaged for each individual marker using a 20X objective on a Nikon Eclipse 90i Imaging Microscope. Quantification of cell types was performed using ImageJ (National Institutes of Health, Bethesda, MD). Cell counts were averaged for each sample and expressed as a percentage of total cells within a 20X field.

Additional sections were triple-labeled with antibodies specific for a pan-macrophage marker (CD68), an M1 marker (CD86), and an M2 marker (CD206) as above. Slides were imaged using a 20X objective at the interface with either single fibers (3 images) or mesh knots (3 images) using a standardized protocol.[28] CD68+CD86+ cells were considered to have an M1 phenotype and CD68+CD206+ cells an M2 phenotype. Cell counts were averaged for each sample and expressed as a percentage of total cells within a 20X field. Additionally, the ratio of M2:M1 cells was calculated. Because of the scarcity of macrophages in the Sham, the ratio of M2:M1 was not reported. The perimeter of the mesh-tissue interface present in each image was calculated by tracing using ImageJ.

ELISA Assay

Frozen tissues were mechanically pulverized and homogenized in a high salt buffer (50 mM Tris Base, 150 mM sodium chloride, and 10ug/mL Halt™ Protease Inhibitor Cocktail, Pierce Biotechnology, Rockford, IL). After centrifugation, supernatants were collected. Using the Bio-Rad DC Protein Assay (Bio-Rad, Hercules, CA), protein concentrations of all extracts were determined so that all sample volumes contained 40 µg of protein. Amounts of pro-inflammatory M1 (TNF-α, and IL-12p70) and anti-inflammatory M2 (IL-10, IL-4) cytokines were assessed using commercially available ELISA assays (Life Technologies, Carlsbad, CA).

Both the concentrations of individual cytokines and the ratio of M2/M1 cytokines ((IL-10+IL-4)/(TNF- α + IL-12)) were calculated.

Statistical Analysis:

Statistical comparisons were made using SPSS 18.0 (SPSS Inc., Chicago, IL, USA). Primate demographic and immunolabeling data were assessed using one-way ANOVA with a Tukey post hoc procedure. As cytokine data were nonparametric, a Kruskal–Wallis test with a Bonferroni adjusted alpha after pairwise comparisons was performed for each group. A Spearman's correlation was used to examine the relationship between the number of M1 and M2 cells and mesh perimeter in each image. A P value of less than 0.05 was used to determine significance.

RESULTS

Animals had similar age, parity, and POP-Q stage (Table 2). The POP-Q staging methods utilized were the same as that utilized in humans adjusted to account for the shorter length of the macaque vagina.[29] Animals in the Restorelle group weighed more than the other groups (P=0.042); however, weight did not correlate with any of the measured outcomes (P>0.36 for all). One animal in the study demonstrated a mesh exposure into the vagina. There were no erosions into adjacent structures..

Histologic Analysis

All samples had an intact and qualitatively normal vaginal epithelium as well as a clearly delineated sub-epithelium, muscular layer, and adventitia (Figure 1). The subepithelial tissues

were histologically similar across all groups, with few differences observed between Sham and mesh implanted animals. The largest differences between samples occurred in the smooth muscle layer as previously described, in which the Gynemesh PS induced the most negative impact. [13] All mesh-implanted animals elicited an inflammatory reaction to individual mesh fibers and around knots consisting of a dense infiltrate of mononuclear cells and formation of a fibrous capsule. The response was highly localized with fewer cells observed with increasing distance from the mesh. Multinucleated giant cells were observed at the surface of some, but not all, fibers and knots, regardless of mesh type. The cells at the mesh-tissue interface were predominantly mononuclear in appearance and few, if any, polymorphonuclear cells (neutrophils) were observed. The adventitial layer in sham-operated animals was qualitatively normal, consisting of well-organized loose connective tissue.

Characterization of the Immune Response to Polypropylene Mesh

CD45+ cells (pan-leukocyte) were observed predominantly at the mesh-tissue interface and in the peri-mesh space in the adventitia with few, if any of these cells within the subepithelium or muscularis of Gynemesh PS-implanted animals indicating a highly localized inflammatory response. CD68+ cells (macrophage) were the immune cell type found in the greatest density immediately surrounding each mesh fiber, while other cells types were fewer in number and found to be located more distantly from the mesh surface (Figure 2). CD45+ cells accounted for 21.4±5.4% of total cells within 20X fields at the mesh-tissue interface. CD68+ cells (macrophages, 10.5±3.9%) were found to be the predominant leukocyte subtype, followed by CD3+ (T-lymphocyte, 7.3±1.7%), CD20+ (B lymphocyte, 3.0±1.2%), and CD117+ (mast, 0.2±0.2%) cells. Although the percentage of macrophages was 44% greater than that of T cells,

no significant statistical differences were observed between these two. Both the percentage of macrophages and T lymphocytes were significantly higher than the percentage of B lymphocytes or mast cells (all P<0.001) (Table 3). No differences in the total number of DAPI+ cells were observed between image sets for each antibody. Few positively labeled cells of any type were observed within the Sham (<5 per 20x field) and, therefore, quantitative analysis of immunolabeled slides was not performed for this group.

Analysis of Macrophage Phenotype

In all implanted animals, the macrophage response to mesh was observed to be predominantly of the M1 phenotype with fewer cells of either phenotype observed with increasing distance from the mesh surface (Figure 3). In areas with individual fibers, the percentage of M1 cells per 20X field was increased in mesh-implanted groups (Gynemesh PS 6.7±2.8%, P=0.003; UltraPro 7.3±2.6%, P=0.002; Restorelle 7.0±3.7%, P=0.008) relative to Sham (0.8±0.7). The percentage of M2 cells was also increased in mesh-implanted groups (Gynemesh PS 3.5±2.2%, P=0.046; UltraPro 4.6±1.5%, P=0.001; Restorelle 4.6±2.1%, P=0.001) relative to Sham (0.07±0.03%). The percentage of M2 cells around individual fibers was similar in lighter weight, higher porosity meshes (UltraPro, P=0.24; Restorelle, P=0.32) as compared to Gynemesh PS. However, the M2/M1 ratio around individual fibers was higher for UltraPro (P=0.033) and Restorelle (P=0.016) as compared to Gynemesh PS. (Table 4). However, the M2/M1 ratio around individual fibers was higher for UltraPro (P=0.033) and Restorelle (P=0.016) as compared to Gynemesh PS. (Table 4)

M1 macrophages around mesh knots were increased in the presence of mesh (Gynemesh PS 8.3±4.7%, UltraPro 9.2±2.8%, Restorelle 8.4±2.6%) relative to Sham (0.09±0.09) (P<0.001).

M2 macrophages also increased with mesh implantation (Gynemesh PS 4.4±2.3%, UltraPro 5.3±1.0%, Restorelle 4.94±1.8%) as compared to Sham (0.09±0.07) (P<0.001). However, in contrast to single fibers, no significant differences in the percentage of M1 and M2 cells or the M2/M1 ratio was observed in areas of mesh knots (Table 5).

The total number of cells within a 20X field was similar in images containing fibers and knots, despite the increased area occupied by knots as compared to fibers. This suggests a more dense inflammatory response around knots as compared to fibers. Though elevated in images with knots, no statistically significant differences in the percentage of M1 and M2 cells was found between images containing fibers and knots for any mesh (P=0.41, 0.18 and 0.51 for Gynemesh PS, UltraPro and Restorelle, respectively). A Spearman's rho test was used to determine whether there was a correlation between mesh perimeter and percentage of M1 and M2 cells in a given image. Results varied by mesh (Table 6), however, examination of correlations across all mesh types demonstrated a significant correlation between mesh perimeter and the percentage of M1 (r=.30, P<0.001) and M2 cells (r=0.23, P=0.006) within a given image.

No statistically significant differences were observed between groups for individual cytokines (all P>0.05) except IL-10 (overall P=0.011) which was 23% higher in the Restorelle as compared to Gynemesh PS (P=0.011). The ratio of M2/M1 cytokines was also increased in Restorelle implanted vagina as compared to Gynemesh PS (P=0.003, Table 7).

COMMENT

The present study sought to define the host inflammatory response to three polypropylene meshes with distinct textile properties following implantation via sacrocolpopexy in the rhesus macaque. The most significant findings were that, while all mesh materials elicited a

predominantly M1 macrophage profile, lower weight, higher porosity meshes (UltraPro and Restorelle) elicited a shift in the M2/M1 macrophage ratio in the area around individual mesh fibers. The concentration of anti-inflammatory cytokine IL-10 was higher in the Restorelle group as compared to Gynemesh PS, with levels approaching that of the Sham operated group, reflecting differences in the overall local microenvironment associated with the implantation of different mesh types.

This shift in the M2/M1 ratio in the area of individual fibers following the implantation of lighter weight, higher porosity meshes, but not following the implantation of a heavier weight, lower porosity mesh is in line with previous observations of abdominal hernia meshes suggesting that "mesh burden", defined as the amount of mesh in contact with tissue, may be critical factor in the immune response to polypropylene mesh. [30-33] These studies show that polypropylene meshes invariably elicit a foreign body reaction, with the amount of chronic inflammation and scarring proportional to pore size, with an increase in the inflammatory response and scarring over time in meshes with decreased pore size. [32] This phenomenon of increased inflammatory scarring with decreased pore size, termed "bridging fibrosis," suggests that increased fiber density (i.e., "mesh burden") corresponds to increased inflammatory and fibrotic reactions due to overlap of the host response to multiple individual fibers in close proximity. In the present study, mesh perimeter was found to be positively correlated with the percentage of both M1 and M2 cells present within a given image, suggesting a link between mesh burden and the host inflammatory response exists for meshes implanted in the vagina.

The results of the present study also suggest that macrophage phenotype may influence tissue integration and/or degradation following mesh implantation. Indeed, corresponding to previous findings that the lighter, wider pore, higher porosity meshes induced fewer negative

effects upon the vagina than did Gynemesh PS, [12-14] the present study observed a higher ratio of M2 to M1 phenotype (macrophage polarization) and increased anti-inflammatory cytokine IL-10 in the lighter but not in the heavier mesh implanted vagina. Similar findings of improved material integration and remodeling associated with increased M2 macrophage populations have been observed in a number of other studies such as those in cardiac, dermal, and orthopedic applications of implantable materials of both biologic and synthetic origin. [18,22-25] In a recent study, [18] fifteen biologically derived surgical meshes were examined for both histologic outcomes and macrophage polarization profile at 14 and 35 days post-implantation in a partial thickness rodent abdominal wall defect model. The study showed that the number of M2 cells and the M2:M1 ratio at 14 days post-implantation were strongly correlated with semi-quantitative scoring of the histomorphologic appearance of the site of implantation at 14 days and were also predictive of the downstream histologic outcome at 35 days post-implantation. Taken together, this suggests that materials which elicit a higher percentage of M2 cells at the tissue interface may be associated with improved tissue integration and fewer complications in the long term.

There were a number of limitations of the present study. First, only one time point was examined, representing a cross sectional snapshot of a highly dynamic inflammatory process. It should also be noted that, due to the presence of an absorbable component poliglecaprolactone 25), the mesh burden associated with the UltraPro mesh and the local composition of the material is also dynamic. Thus, the host response to UltraPro may have a transient component which is not present in the other mesh materials. While statistically significant differences were observed between materials at 90 days, the magnitude of these differences was relatively small. Evaluation of macrophage phenotype at earlier times may have yielded larger differences, but is

likely not possible in a primate model due to cost and ethical considerations. Second, only one marker of M1 and M2 macrophage phenotypes was used in the present study. It is well known that macrophage phenotype occurs along a spectrum between M1 and M2 with multiple intermediate phenotypes.[21] While this represents the first such attempt to measure macrophage polarization in response to material implantation within the vagina, future studies are needed to better define both the phenotype and the function of the cells participating in the host response to implanted mesh to better understand their impact upon tissue integration versus degradation and the occurrence of complications in the long term.[34,35] Third, the present study describes a macrophage centered approach to the evaluation of the host response at the mesh-tissue interface. Future analyses could specifically evaluate the inflammatory reaction as a function of distance from the mesh surface or within pore spaces. This may be particularly important given that additional cell types, including a notable presence of T-lymphocytes, was observed with increasing distance from the mesh surface. Lastly, only mesh introduced by sacrocolpopexy was examined in the present study. Future studies should examine whether there are differences in the host response between mesh introduced by sacrocolpopexy versus transvaginally, and attempt to correlate the findings to the differences in rates of complications which have been observed for these two procedures.

In conclusion, the host response to polypropylene mesh consists predominantly of macrophages polarized to a pro-inflammatory M1 phenotype at 12 weeks post-surgery. However, implantation of lighter weight, higher porosity mesh generally attenuated the pro-inflammatory M1 response. These findings correlate with those of a previous study demonstrating that lighter weight, higher porosity mesh was also associated with fewer negative effects upon vaginal tissue quality. This suggests that the chronic M1 pro-inflammatory

response to mesh may drive tissue degradation eventually leading to mesh exposures over time similar to what is observed clinically; however, additional work is required to establish a causal relationship. An improved scientific understanding of the mechanisms of the host response to synthetic mesh materials placed in the vagina has the potential to significantly affect the design of next generation mesh materials, inform clinical practices and improve outcomes in pelvic floor repair.

CLINICAL IMPLICATIONS

- Regardless of mesh type or textile properties, the host response to mesh consists of predominantly of M1 pro-inflammatory macrophages.
- Implantation of lighter weight, higher porosity mesh generally attenuated the pro-inflammatory response, suggesting a link between mesh burden and the host inflammatory response.
- These findings correlate with those of a previous study demonstrating that lighter weight, higher porosity mesh was also associated with fewer negative effects upon vaginal tissue quality.
- This suggests that the chronic M1 pro-inflammatory response to mesh may drive tissue degradation eventually leading to mesh exposures over time similar to what is observed clinically.

REFERENCES

1. Subak LL, Waetjen LE, van den Eeden S, Thom DH, Vittinghoff E, Brown JS. Cost of pelvic organ prolapse surgery in the United States. Obstet gynecol. 2001;98:646-51.

2. Boyles SH, Weber AM, Meyn L. Procedures for pelvic organ prolapse in the United States, 1979-1997. Am J Obstet Gynecol. 2003;188:108-15.

3. Wu JM, Kawasaki A, Hundley AF, Dieter AA, Myers ER, Sung VW. Predicting the number of women who will undergo incontinence and prolapse surgery, 2010 to 2050. Am J Obstet Gynecol. 2011;205:230 e1-5.

4. Barber MD, Brubaker L, Burgio KL, et al. Comparison of 2 transvaginal surgical approaches and perioperative behavioral therapy for apical vaginal prolapse: the OPTIMAL randomized trial. JAMA. 2014;311:1023-34.

5. Olsen AL, Smith VJ, Bergstrom JO, Colling JC, Clark AL. Epidemiology of surgically managed pelvic organ prolapse and urinary incontinence. Obstet gynecol. 1997;89:501-6.

6. Jonsson Funk M, Edenfield AL, Pate V, Visco AG, Weidner AC, Wu JM. Trends in use of surgical mesh for pelvic organ prolapse. Am J Obstet Gynecol. 2013;208:79 e1-7.

7. Altman D, Vayrynen T, Engh ME, et al. Anterior colporrhaphy versus transvaginal mesh for pelvic-organ prolapse. N Eng J Med. 2011;364:1826-36.

8. Diwadkar GB, Barber MD, Feiner B, Maher C, Jelovsek JE. Complication and reoperation rates after apical vaginal prolapse surgical repair: a systematic review. Obstet gynecol. 2009;113:367-73.

9. Feiner B, Jelovsek JE, Maher C. Efficacy and safety of transvaginal mesh kits in the treatment of prolapse of the vaginal apex: a systematic review. BJOG. 2009;116:15-24.

10. Maher CM, Feiner B, Baessler K, Glazener CM. Surgical management of pelvic organ prolapse in women: the updated summary version Cochrane review. Int Urogynecol J. 2011;22:1445-57.

11. (FDA) FaDA. Urogynecologic Surgical Mesh: Update of the Safety and Effictiveness of Transvaginal Placement for Pelvic Organ Prolapse.: FDA Administration E.

12. Feola A, Abramowitch S, Jallah Z, et al. Deterioration in biomechanical properties of the vagina following implantation of a high-stiffness prolapse mesh. BJOG. 2013;120:224-32.

13. Liang R, Abramowitch S, Knight K, et al. Vaginal degeneration following implantation of synthetic mesh with increased stiffness. BJOG. 2013;120:233-43.

14. Liang R, Zong W, Palcsey S, Abramowitch S, Moalli PA. Impact of prolapse meshes on the metabolism of vaginal extracellular matrix in rhesus macaque. Am J Obstet Gynecol. 2015 Feb;212(2):174.e1-7.

15. Mistrangelo E , Mancuso S, Nadalini C, Lijoi D, Costantini S. Rising use of synthetic mesh in transvaginal pelvic reconstructive surgery: a review of the risk of vaginal erosion. J Minim Invasive Gynecol. 2007 Sep-Oct;14(5):564-9.

16. Kohli N, Walsh PM, Roat TW, Karram MM. Mesh erosion after abdominal sacrocolpopexy. Obstet Gynecol. 1998 Dec;92(6):999-1004.

17. Brown BN, Badylak SF. Expanded applications, shifting paradigms and an improved understanding of host-biomaterial interactions. Acta Biomater. 2013;9:4948-55.

18. Brown BN, Londono R, Tottey S, et al. Macrophage phenotype as a predictor of constructive remodeling following the implantation of biologically derived surgical mesh materials. Acta Biomater. 2012;8:978-87.

19. Mantovani A, Sica A, Sozzani S, Allavena P, Vecchi A, Locati M. The chemokine system in diverse forms of macrophage activation and polarization. Trends Immunol. 2004;25:677-86.

20. Mills CD, Kincaid K, Alt JM, Heilman MJ, Hill AM. M-1/M-2 macrophages and the Th1/Th2 paradigm. J Immunol. 2000;164:6166-73.

21. Mosser DM, Edwards JP. Exploring the full spectrum of macrophage activation. Nat Rev Immunol. 2008;8:958-69.

22. Madden LR, Mortisen DJ, Sussman EM, et al. Proangiogenic scaffolds as functional templates for cardiac tissue engineering. Proc Natl Acad Sci USA. 2010;107:15211-6.

23. Rao AJ, Gibon E, Ma T, Yao Z, Smith RL, Goodman SB. Revision joint replacement, wear particles, and macrophage polarization. Acta biomater. 2012;8:2815-23.

24. Sussman EM, Halpin MC, Muster J, Moon RT, Ratner BD. Porous implants modulate healing and induce shifts in local macrophage polarization in the foreign body reaction. Ann Biomed Eng. 2014;42:1508-16.

25. Brown BN, Ratner BD, Goodman SB, Amar S, Badylak SF. Macrophage polarization: an opportunity for improved outcomes in biomaterials and regenerative medicine. Biomaterials. 2012;33:3792-802.

26. Feola A, Barone W, Moalli P, Abramowitch S. Characterizing the ex vivo textile and structural properties of synthetic prolapse mesh products. Int Urogynecol J. 2013;24:559-64.

27. Maher C, Feiner B, Baessler K, Schmid C. Surgical management of pelvic organ prolapse in women. Cochrane Database Syst Rev. 2013;4:CD004014.

28. Wolf MT, Dearth CL, Ranallo CA, et al. Macrophage polarization in response to ECM coated polypropylene mesh. Biomaterials. 2014;35:6838-49.

29. Feola A, Abramowitch S, Jones K, Stein S, Moalli P. Parity impacts vaginal mechanical properties and collagen structure in rhesus macaques. Am J Obstet Gynecol. 2010;203:595.e1-595.e8.

30. Conze J, Rosch R, Klinge U, et al. Polypropylene in the intra-abdominal position: influence of pore size and surface area. Hernia. 2004;8:365-72.

31. Klinge U, Junge K, Stumpf M, Ap AP, Klosterhalfen B. Functional and morphological evaluation of a low-weight, monofilament polypropylene mesh for hernia repair. J Biomed Mater Res. 2002;63:129-36.

32. Klinge U, Klosterhalfen B, Birkenhauer V, Junge K, Conze J, Schumpelick V. Impact of polymer pore size on the interface scar formation in a rat model. J Surg Res. 2002;103:208-14.

33. Klinge U, Park JK, Klosterhalfen B. 'The ideal mesh?'. Pathobiology. 2013;80:169-75.

34. Brown BN, Sicari BM, Badylak SF. Rethinking regenerative medicine: a macrophage-centered approach. Front Immunol. 2014;5:510.

35. Murray PJ, Allen JE, Biswas SK, et al. Macrophage activation and polarization: nomenclature and experimental guidelines. Immunity. 2014;41:14-20.

TABLES

Table 1. Mechanical and structural characteristics associated with each mesh.

	Gynemesh (Ethicon)	UltraPro (Ethicon)	Restorelle (Coloplast)
Weight (g/m2)	44	31	19
Pore Size (μm)	2240	4000+*	2370
Porosity (%)	64±2.1	69 ± 1.8	78 ± 3.0
Stiffness (N/mm)	28±2.7	22±2.8	11±0.89

*UltraPro contained a resorbable component (poliglecaprolactone 25) in addition to polypropylene allowing it to have very large pores (4mm) when this component is resorbed. Values reported with resorbable component dissolved.
Adapted from references #12 and 26.

Table 2. Demographic data collected (age, weight, gravidity and parity).

Groups	Age, y[a]	Parity[b]	Weight, kg[a]	POP-Q stage[b]
Sham	12.6 ± 2.8	3 (2, 6)	*7.3 ± 1.4	0 (0, 1)
Gynemesh	12.9 ± 2.2	4 (3.8, 5)	8.2 ± 1.6	0 (0, 0)
UltraPro	13.0 ± 2.2	3.5 (2, 5.8)	7.8 ± 1.4	0 (0, 0.25)
Restorelle	13.8 ± 1.7	5 (3, 5.5)	*10.0 ± 2.8	0.5 (0, 1.3)
P value[c]	0.780	0.970	0.042	0.700

[a] Mean ± SD, [b] Median (first quartile, second quartile), [c] Comparison of overall P value among groups, * Denotes statistical significance between groups (P<0.05)

Table 3. Total number of cells and percent surface marker postive cells in a 20X field.

Treatment (Gynemesh)	Total Number of Cells (per 20X field)	% of Positive Cells (per 20X field)
CD45	514±121	21.4±5.4
CD68	510±108	[c]10.5±3.9
CD3	510±114	[d]7.3±1.7
CD20	509±109	3.0±1.2
CD117	508±121	0.2±0.2
P value	1.00[a]	<0.001[b]

[a] Comparison of p-value among groups, significant difference if p<0.05; b Comparison between CD68, CD3, CD20, and CD117, [c] Significance seen between CD68 and CD20 and CD68 and CD117; [d] Significance seen between CD3 and CD20 and CD3 and CD117.

Table 4. total number of cells, percent of positive cells and ratio of m2/m1 macrophages seen in a 20X field (fiber)

Total Number of Cells, Percent of Positive Cells and Ratio of M2/M1 Macrophages in a 20x Field (Fiber)				
Treatment	**Total Number of Cells**	**% of M1 Positive Cells**	**% of M2 Positive Cells**	**Ratio M2/M1**
Sham	696±370	[b]0.8±0.7	[b]0.1±0.0	-
Gynemesh	642±215	6.8±2.8	3.5±2.2	[c]0.52±0.14
UltraPro	768±232	7.3±2.6	4.6±1.5	0.66±0.08
Restorelle	610±291	7.0±3.7	4.6±2.1	0.67±0.09
P value[a]	0.700	<0.001	<0.001	<0.001

[a] Comparison of p-value among groups, significant difference if p<0.05; [b] Significance seen between Sham and Gynemesh, Sham and UltraPro and Sham and Restorelle; [c] Significance seen between Gynemesh and UltraPro and Gynemesh and Restorelle

Table 5. Total number of cells, percent of positive cells and ratio of m2/m1 macrophages seen in a 20X field (knot)

Total Number of Cells, Percent of Positive Cells and Ratio of M2/M1 Macrophages in a 20x Field (Knot)				
Treatment	**Total Number of Cells**	**% of M1 Positive Cells**	**% of M2 Positive Cells**	**Ratio M2/M1**
Sham	679±327	[a]0.1±0.1	[a]0.1±0.0	-
Gynemesh	630±230	8.3±4.7	4.4±2.3	0.57±0.11
UltraPro	722±214	9.2±2.8	5.3±1.0	0.61±0.18
Restorelle	575±104	8.4±2.6	4.9±1.8	0.60±0.11
P value[e]	0.620	<0.001	<0.001	<0.001

[a] Comparison of p-value among groups, significant difference if $p<0.05$; [a] Significance seen between Sham and Gynemesh, Sham and UltraPro and Sham and Restorelle

Table 6. Correlation between percentage of positive cells and mesh area in a 20X image

Correlation Between Percentage of Positive Cells and Mesh Area in a 20X Image				
	% M1 Cells vs. Area		**% M2 Cells vs. Area**	
	Correlation Coefficient	**P value**	**Correlation Coefficient**	**P value**
Gynemesh	0.39	0.006	0.44	0.002
UltraPro	0.35	0.015	0.23	0.113
Restorelle	0.24	0.098	0.22	0.136
All Mesh	0.30	0.001	0.23	0.006

Table 7. Individual and ratio values of anti- and pro-inflammatory cytokines

Individual and Ratio Values of Anti- and Pro-inflammatory Cytokines					
Groups	**IL-10**[a]	**IL-4**[a]	**TNF-α**[a]	**IL-12p70**[a]	**(IL-10+IL-4)/ (TNF-α+IL-12p70)**[b]
Sham	1.30±0.31	0.33±0.01	0.38±0.11	0.26±0.06	2.58±0.52
Gynemesh	1.03±0.20	0.29±0.08	0.33±0.12	0.27±0.05	*2.17±0.78
UltraPro	1.12±0.22	0.27±0.11	0.28±0.15	0.23±0.07	3.01±0.90
Restorelle	1.27±0.22	0.263±0.05	0.26±0.05	0.30±0.15	*3.36±0.60
P value[c]	0.014	0.358	0.084	0.386	0.004

[a] pg/µg total protein, mean ± standard deviation; [b] unitless, mean ± standard deviation; [c] comparison of overall P value among groups, * Denotes statistical significance between groups ($P<0.05$)

FIGURE LEGENDS

Figure 1: Representative histologic section (hematoxylin and eosin) taken from Sham (A) and Gynemesh (B) groups. The top panel contains a full view of the histologic section at 10X magnification (scale bar = 250 μm). Bottom panel shows higher magnification images of the subepithelial connective tissues, muscularis layer and the adventitia (A) or mesh-tissue interface (B) (20x magnification, scale bar = 100 μm). The histomorphologic appearance of the response to Gynemesh was characteristic of the response observed in all mesh implanted groups. A dense population of mononuclear and multinucleated giant cells can be observed at the mesh-tissue interface, decreasing in number with increasing distance from the mesh surface. Box in (B) indicates a mesh knot, and arrow indicates a mesh fiber.

Figure 2: Immunofluorescent labeling of cells participating in the host response to implanted mesh. Antibodies for CD45 (pan-leukocyte), CD68 (macrophage), CD3 (T lymphocyte), CD20 (B lymphocyte), and CD117 (mast cell) markers were used (red). DAPI (blue) was used to label nuclei. Positively labeled cells were predominantly located at the mesh surface, with fewer cells with increasing distance. All images at 40X magnification, scale bar = 100 μm.

Figure 3: Immunofluorescent labeling with antibodies to CD68 (Pan-macrophage, red), CD86 (M1 macrophage, orange), CD206 (M2 macrophage, green) and DAPI (nuclei, blue) is shown. Few positive cells were observed in sham-operated animals (not shown). Predominance of the M1 macrophage response was observed in Gynemesh PS, UltraPro and Restorelle groups. Combined fluorescent channels are shown in the top panel, and individual channels in the bottom panel. All images at 20X magnification, scale bars = 100 μm.

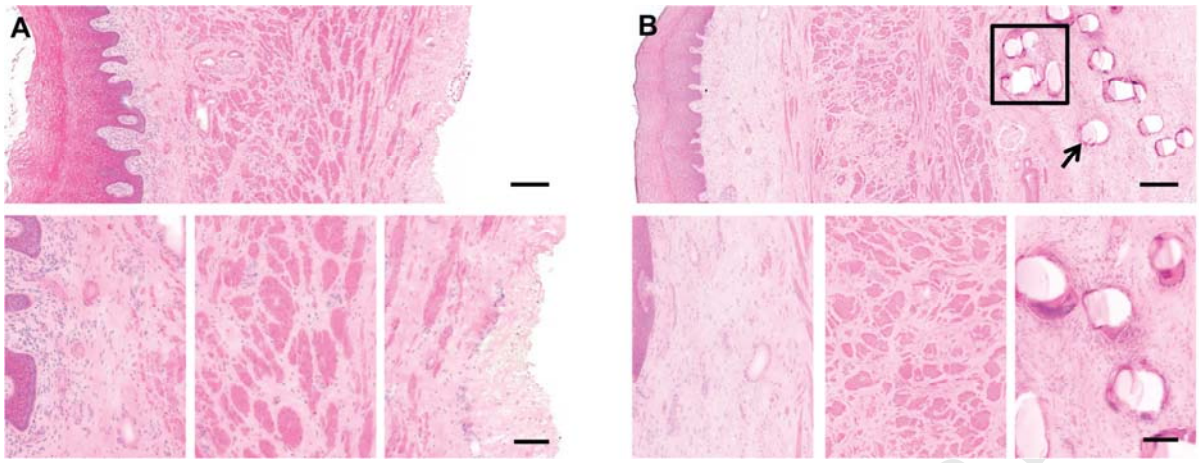

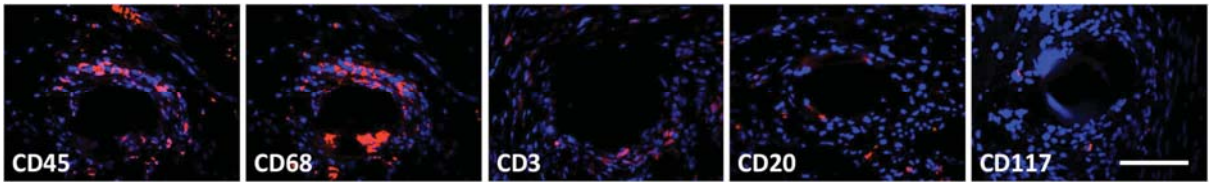

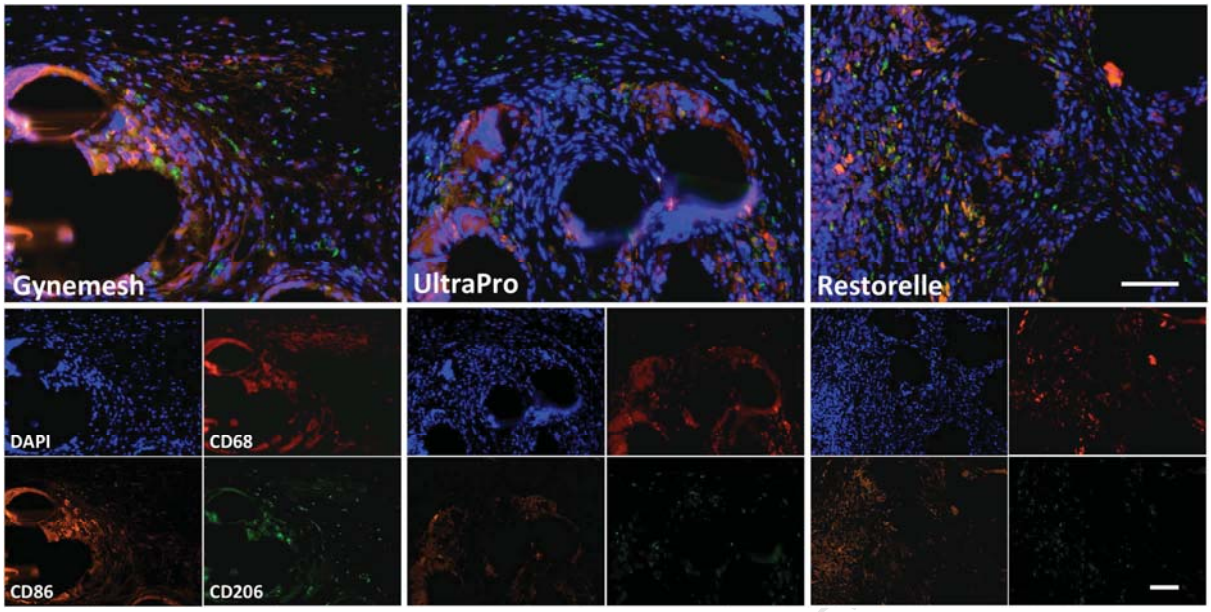

Table III: Antibodies used in immunofluorescence labeling

Primary Antibody				
Name	**Dilution**	**Catalog Number**	**Clonality**	**Company**
Rabbit Anti-CD45	1:600	ab10558	Polyclonal	abcam
Mouse Anti-CD68	1:100	ab955	Monoclonal	abcam
Rabbit Anti-CD3	1:50	A0452	Polyclonal	DAKO
Rabbit Anti-CD20	1:50	ab27093	Polyclonal	abcam
Rabbit Anti-CD117	1:50	ab32363	Monoclonal	abcam
Rabbit Anti-CD86	1:150	ab53004	Monoclonal	abcam
Goat Anti-CD206	1:150	sc-34577	Polyclonal	Santa Cruz
Secondary Antibody				
Name	**Dilution**	**Catalog Number**	**Wavelength**	**Company**
Alexa 594 Donkey anti-Mouse	1:100	A21203	590/617	Invitrogen
Alexa 568 Donkey anti- Rabbit	1:50 (CD3, CD20 & CD117) 1:200 (CD45)	A10042	578/603	Invitrogen
Alexa 488 Donkey anti- Goat	1:250 (CD206)	A11055	488/519	Invitrogen
Alexa 647 Donkey anti- Rabbit	1:250 (CD86)	A31573	650/668	Invitrogen